ANNUAL REPORT

TO

OFFICE OF NAVAL RESEARCH

Contract USN 00014-96-I0913

May 1999

EFFECTS OF POLLUTANATS AND MICROORGANISMS ON THE ABSORPTION OF ELECTROLYTIC HYDROGEN IN IRON

H.W. Pickering

Department of Materials Science and Engineering
The Pennsylvania State University
University Park, PA 16802

PENN STATE

REPORT DOCUMENTATION PAGE

Form Approved
OMB No. 0704-0188

1. AGENCY USE ONLY (Leave blank)	2. REPORT DATE	3. REPORT TYPE AND DATES COVERED
	May 1999	Annual

4. TITLE AND SUBTITLE

Effects of Pollutants and Microorganisms on the Absorption of Electrolytic Hydrogen in Iron

5. FUNDING NUMBERS

USN 00014-96-I-0913

6. AUTHOR(S)

Howard W. Pickering

7. PERFORMING ORGANIZATION NAME(S) AND ADDRESS(ES)

The Pennsylvania State University
Department of Materials Science and Engineering
326 Steidle Building
University Park, PA 16802

8. PERFORMING ORGANIZATION REPORT NUMBER

9. SPONSORING/MONITORING AGENCY NAME(S) AND ADDRESS(ES)

Program Officer
ATTN: A. John Sedriks, ONR 332
Office of Naval Research
Ballston Centre Tower One
800 North Quincy Street
Arlington, VA 22217-5660

10. SPONSORING/MONITORING AGENCY REPORT NUMBER

11. SUPPLEMENTARY NOTES

12a. DISTRIBUTION/AVAILABILITY STATEMENT

Approved for public release; distribution is unlimited.

12b. DISTRIBUTION CODE

13. ABSTRACT *(Maximum 200 words)*

The objective of this research is to define conditions under which pollutants, in particular those produced by bacteria such as sulfide end products of the SRB, affect the amount of hydrogen absorbed by iron/ steel. Thiosulfate in neutral solutions enhances the hydrogen evolution reaction (HER) and the hydrogen absorption reaction (HAR) on iron. A concentration of 10mM thiosulfate increases the hydrogen absorption rate by 3 fold. This promoting effect of thiosulfate in neutral solutions is due to its thermodynamic instability and its reduction to hydrogen sulfide. Iodide ion as one of the constituents of seawater has a different behavior towards both the HER and HAR on iron. It inhibits the HER while enhancing the HAR. Analysis of the results using the IPZ model shows that iodide ions inhibit the HER by decreasing its discharge rate constant and the hydrogen surface coverage. On the other hand, iodide ions enhance the HAR by increasing the absorption-desorption constant.

14. SUBJECT TERMS

Key words: hydrogen absorption, hydrogen evolution, steel, pollutants, sulfide, SRB, MIC, iodide, modeling

15. NUMBER OF PAGES

16. PRICE CODE

17. SECURITY CLASSIFICATION OF REPORT	18. SECURITY CLASSIFICATION OF THIS PAGE	19. SECURITY CLASSIFICATION OF ABSTRACT	20. LIMITATION OF ABSTRACT

Introduction

The hydrogen absorption reaction (HAR) has gained increasing interest in view of its effects on the structural integrity of metals. Hydrogen absorption occurs as a direct result of the hydrogen evolution reaction (HER). The HER is a ubiquitous reaction in aqueous solutions, occurring during corrosion, electroplating, cathodic protection, pickling, etc. Certain species and microorganisms in the aqueous environments can significantly affect the extent of hydrogen absorption. Some species inhibit hydrogen absorption and hydrogen evolution, e.g., benzotriazole and benzonitrile (1,2). Others inhibit the HER while enhancing the HAR, e.g., iodide ions and aminotriazole (1,3,4). Still others are species that enhance both reactions, e.g., H_2S. The Latter can come as a direct reduction of sulfates by sulfate reducing bacteria (SRB).

The SRB are anaerobic bacteria that develop quickly in environments such as those encountered in the marine environments and fuel and waste water treatment tanks (5-8). They facilitate the action of differential aeration which results in severe corrosion. The hydrogen that comes out of the corrosion process is subsequently used by the

SRB to reduce sulfate ions (8): $10H + SO_4^{2-} \rightarrow H_2S + 4H_2O$. The formation of H_2S in this process accelerates corrosion and drastically enhances hydrogen absorption.

The ongoing research plan is to investigate the kinetics of the HER and HAR on iron in acidic solution in the presence of site blocking elements (SBE) such as iodide ions. These site blocking elements are capable of enhancing the HER while inhibiting the HAR. Data were collected on iron in acidic solutions in the absence and presence of iodide ions, using the electrochemical hydrogen permeation cell (9,10). The data were subsequently analyzed using the IPZ model (11) to extract the thermodynamic parameters such as the hydrogen surface coverage, θ_H, and the kinetic parameters (rate constants) of both the HER and HAR. The research plan also investigated the effect of thiosulfate on the HER and HAR on iron in neutral solutions. This is of particular importance because of the severe corrosion damage that thiosulfate also imparts to iron base alloys, in the form of pitting and crevice corrosion and stress corrosion cracking (12-15). It is also because that thiosulfate is one of the end products of SRB(16). In fact, its presence in the water cooling system led to the failure of the Three Mile Island nuclear reactor in Pennsylvania in 1981(17).

Experimental

The electrochemical hydrogen permeation cell was similar to that used by Devanathan and Stachurski (9) and by Frumkin (10). The cell was used to collect data on both the HER and HAR on iron membranes of thickness 0.25 mm in acidic solution of 0.1N H_2SO_4 + 0.9 N Na_2SO_4. The samples were annealed in pure hydrogen at 900°C for 2hrs and furnace cooled in the same atmosphere. All solutions were prepared from analytical grade chemicals and double distilled water. Before admitting the solutions to the cell, they were pre-electrolyzed at 3 mA for 2 hours to remove impurities that could otherwise affect the quality of the data. The solutions were subsequently de-aerated with hydrogen. Further details about the experimental setup can be found elsewhere (18).

Results

A- The Effect of Iodide Ions on the Kinetics of Hydrogen Absorption by Iron

Fig.1 shows the effect of iodide ion concentration on the relation between the steady state hydrogen permeation current density and the cathodic potential at the charging side of the membrane. Iodide ions enhance hydrogen absorption, i.e., the steady state hydrogen permeation

current density increases at a given cathodic potential with increasing concentration of iodide ion in the solution. Also, the well established general relation between cathodic potential and permeation for all metal/electrolyte systems was observed, i.e., at a certain concentration of iodide ions, greater cathodic potentials produce larger permeation currents (1,3). The increase in the steady state hydrogen permeation current with increasing concentration of iodide ions is accompanied by a decrease in the rate of the HER as shown by Fig.2, which indicates that the iodide ions inhibit the HER.

The above results show that iodide ions inhibit the HER while enhancing the HAR. To understand the mechanism by which iodide raises i_∞ while decreasing i_c (at constant E), one has to also know the values of the hydrogen surface coverage and the different rate constants involved in both reactions in the absence and presence of the iodide ions. We used the IPZ model (11) which has been successfully used by many authors to analyze the kinetics of both reactions during electroplating (19) and during cathodic polarization in the presence of inhibitors or promoters in the aqueous environment (20,21).

The IPZ model describes the kinetics of both the HER and HAR in a set of simple analytical equations which when solved, can fully describe their kinetics. Details about the model can be found elsewhere (11). The IPZ model describes the HER in terms of a coupled discharge Tafel recombination mechanism, i.e.,

$$H^+ + e^- + M \xrightarrow{k_1} M\text{-}H_{ads} \qquad (1)$$

$$M\text{-}H_{ads} + M\text{-}H_{ads} \xrightarrow{k_2} 2M + H_2 \qquad (2)$$

where $M\text{-}H_{ads}$ refers to an adsorbed hydrogen atom on the metal surface and k_1 and k_2 are the rate constants of the discharge and recombination steps of the HER. This adsorbed hydrogen, $M\text{-}H_{ads}$, is also considered to be involved in the hydrogen absorption reaction, i.e.,

$$M\text{-}H_{ads} \underset{k_{des}}{\overset{k_{abs}}{\Leftrightarrow}} M\text{-}H_{abs} \qquad (3)$$

where $M\text{-}H_{abs}$ refers to the absorbed hydrogen atom inside the metal lattice and k_{abs} and k_{des} refer to the rate constants of the forward and backward directions of reaction 3. The basic equations of the IPZ model are summarised as follows:

$$i_c = Fk_1C_{H^+}(1-\theta_H)\ \exp(-a\alpha\eta) \qquad (4)$$

$$i_c\exp(a\alpha\eta) = i_o'(1-\theta_H) \qquad (5)$$

$$i_r = Fk_2\theta^2_H \quad (6)$$

$$i_\infty = \frac{FDC^o}{L} \quad (7)$$

$$i_\infty = Fk_{abs}\theta_H - Fk_{des}C^o \quad (8)$$

$$i_\infty = Fk''\theta_H \quad (9)$$

$$i_\infty = k'' \sqrt{\frac{F}{k_2}} \sqrt{i_r} \quad (10)$$

$$i_c \exp(a\alpha\eta) = i_o' - \frac{i_o'}{Fk''} i_\infty \quad (11)$$

where C_{H+} is the hydrogen ion concentration, a=F/RT, α is the transfer coefficient of the HER, η is the hydrogen overpotential, θ_H is the hydrogen surface coverage, $i_o' = Fk_1 C_{H+}$, i_r is the recombination current of the HER, i_∞ is the steady state hydrogen permeation current density, D is the hydrogen diffusion coefficient in the metal, C^o is the steady state concentration of the absorbed hydrogen in the metal at the charging surface, L is the membrane thickness and k" is the thickness dependant absorption-desorption constant which is defined as $k'' = \frac{k_{abs}}{1 + k_{des}\frac{L}{D}}$. The left hand side of Eq.5 is referred to as the charging function and has units of A cm^{-2}. Equation 11 is the backbone of the IPZ model as it represents a straight line relation between the charging function, $i_c \exp(a\alpha\eta)$ and the steady state hydrogen permeation current density, i_∞. The slope of this relation is $-\frac{i_o'}{Fk''}$ while the intercept equals i_o'. Accordingly, the value of k'' can be obtained and,

subsequently, the hydrogen surface coverage can be evaluated from Eq.9. Moreover, the value of the recombination rate constant, k_2, can be calculated from the slope of the relation between the i_∞ and $\sqrt{i_r}$ after substituting for the value of k'' evaluated from the model. The discharge rate constant can also be evaluated from the value of i_o' (the intercept of Eq.11).

Fig.3 shows the relation between the steady state permeation current density and the square root of the recombination current density at different iodide ion concentrations for an iron membrane of thickness 0.25mm in 0.1N H_2SO_4 + 0.9N Na_2SO_4. This figure shows fairly straight lines passing through the origin, indicating that the HER occurred by the coupled discharge-Tafel recombination mechanism (11) in both the absence and presence of iodide ions. The slopes of the lines in Fig.3 increase as the iodide ion concentration increases. An increase in the slope of these straight lines might result from an increase in k" and/or a decrease in k_2 (see Eq.10).

The Tafel slope for the blank solution was 120 mV corresponding to a transfer coefficient, α = 0.5. This value was used to calculate the charging function, i_c

$\exp(a\alpha\eta)$, under various conditions. Fig. 4 shows the relation between the charging function and the steady state permeation current at different iodide concentrations. The relations are satisfactory straight lines with negative slopes in agreement with the prediction of Eq.11. The magnitudes of the slope decrease sharply with increase in the iodide ion concentration. The decrease in the slope of the lines can be brought about by an increase in k'' and/or a decrease in i_o', see Eq.11. The intercepts of the lines in Fig.4 with the y-axis give the values of the exchange current density of the HER, $i_o' = i_o\ (1-\theta_H^e) \approx i_o$ for cases where $\theta_H^e << 1$. The discharge rate constant was then calculated from the relation $i_o'=Fk_1C_{H+}$ from Eqs.4 and 5, and the slopes and intercepts of the lines in Fig.4 were analyzed for the values of the absorption-desorption constant, k''(according to Eq.11). The values of k'' at different iodide ion concentrations were then used to estimate the recombination rate constant of the HER, k_2, from the slopes of the lines in Fig.3, in accord with Eq.10. Table.1 shows values for i_o, k_1, k_2 and k'' at different iodide ion concentrations. The results show that iodide ions inhibit the HER by decreasing the value of the discharge rate constant, k_1. Similar results were found in

the literature for the effect of organic inhibitors on the discharge rate constant of the HER (20). On the other hand, iodide promotes the HAR by increasing the absorption-desorption constant, k'', Eq.9.

The results in Table.1 show that the iodide ions also slightly increase the recombination rate constant of the HER, k_2. The latter could lead to a decrease in the hydrogen surface coverage. The values of k'' were used to estimate the hydrogen surface coverage using Eq.9 at different potentials and iodide concentrations. Fig.5 gives the relations between the coverage and potential. For the blank solution the coverage increases with an increase in the potential in the cathodic direction as expected, which confirms results obtained earlier by other authors for various systems (19-23). This figure also reveals that the hydrogen surface coverage decreases with increasing concentration of iodide ions in the charging solution. The decrease in the hydrogen surface coverage (Fig.5) dominates over the slight increase in the recombination rate constant of the HER, k_2, (Table.1). For example, inserting the value of θ_H =0.325 and $k_2=3.79\times10^{-8}$ for an iodide ion concentration of 50mM (E=-0.7V(SCE)) into Eq.6 yields a three fold decrease in the recombination current over that of the blank solution.

B- The Effect of thiosulfate on the Hydrogen Absorption by Iron from Neutral Solutions

Fig.6 shows hydrogen permeation transients obtained on an iron membrane of thickness 0.25mm in a neutral solution of 0.5M Na_2SO_4. This figure shows that thiosulfate in the neutral medium increases the rate of hydrogen absorption within iron. A concentration of 0.1 mM of thiosulfate increases i_∞ by about 2 fold while the 10 mM increases it by about 3 folds. This increase in the hydrogen absorption reaction in the neutral solution was accompanied by an increase in the HER kinetics. Fig.7 shows polarization plots obtained on iron in 0.5M Na_2SO_4 at different thiosulfate ion concentrations. This figure reveals that thiosulfate enhances the HER by decreasing the hydrogen overpotential at the same value of the applied cathodic charging current.

The mechanism by which thiosulfate enhances both the HER and HAR on iron is related to its thermodynamic instability and its reduction to hydrogen sulfide as follows

$$S_2O_3^{2-} + 6H^+ + 4e^- \rightarrow 2S + 3H_2O \quad (12)$$

$$S + 2H^+ + 2e^- \rightarrow H_2S \quad (13)$$

The formation of hydrogen sulfide is known to give rise to an enhanced hydrogen absorption and evolution rates.

Conclusions

Iodide ions in acidic solutions inhibit the HER on iron while enhancing the HAR. Analysis of the experimental results using the IPZ model shows that iodide ions lead to the following effects:

a- A decrease in the hydrogen surface coverage, θ_H,

b- A decrease in the discharge rate constant of the HER, k_1, and hence in the exchange current density, i_o.

c- An increase in the absorption-desorption constant of the HAR, k'' and

d- A small but detectable increase in the recombination rate constant of the HER, k_2.

Accordingly, the above data and IPZ results reveal that the increase in the hydrogen absorption rate in the presence of iodide ions is caused by an increase in the absorption-desorption constant, k". This increase in k'' dominates over the decrease in the hydrogen surface coverage, θ_H, (caused by the decrease in k_1 and increase in k_2) in Eq.9 and leads to the enhanced hydrogen absorption. The inhibiting effect of iodide ions on the HER is due to the decrease in k_1 as revealed by evaluating Eq.4, and by the decrease in the θ_H as revealed by evaluating Eq.6.

Thiosulfate in neutral solutions enhances the hydrogen evolution and absorption reactions on iron. The effect was attributed to its reduction to hydrogen sulfide which is known to enhance hydrogen absorption into iron base alloys.

References

1. J.O'M Bockris, J.McBreen, and L.Nanis, J.Electrochem.Soc.,**112**,1025(1965).
2. D.L.Dull and K.Nobe,Corrosion,**35**,535(1979).
3. E.G.Dafft, K.Bohnenkamp and H.J.Engell, Corros. Sci., **19**,591(1979).
4. N.Subramanyan, K.Balakrishnan, B.Sathianan, Proceeding of the 3rd European Symposium on Corrosion Inhibitors, **5**, 591-616 (1970).
5. R.E. Tantall, Mater. Perform., **8**,32(1981).
6. J.W. Costerton, Mater. Perform., **23**,31(1984).
7. A.K. Tiller, in Corrosion Processes, R.N. Parkins, Ed., p.115, Applied Science Publishers, New York(1982).
8. J.M.Genin, A.A. Olowe, B. Resiak, N.D.Benbouzid, S.L. Haridon, M. Confente and D. Prieur, in Progress in the Understanding and Prevention of Corrosion, J.M. Costa and A.D. Mercer, editors, p.1185, The institute of Materials(1993).
9. M. A. Devanathan and Z. Stachurski, Proc. Roy. Soc.Chem., **A270**, 90 (1962).
10. A. N. Frumkin and N. Aladyalova, Acta Physicochim (USSR), **19**, 1 (1944).
11. R.N.Iyer, H.W.Pickering and M.Zamanzadeh, J.Electrochem.Soc., **136**,2463(1989).
12. R.C.Newman, Corrosion, **41**,450 (1985).
13. S.J.Mulford and D. Tromans, Corrosion, **44**, 891(1988).
14. H.H.Horowitz, Corr.Sci., **23**,353(1983).
15. A.Garner, Pulp and Paper Canada, **83**,20(1982).
16. P. Marcus, in Corrosion Mechanisms in Theory and Practice, P. Marcus and J. Oudar, Editors, p.239, Marcel and Dekker, New York(1995).
17. D. A. Jones in Principle and Prevention of Corrosion 1992, page.371.
18. M.H.Abd Elhamid, B.G.Ateya and H.W. Pickering, J.Electrochem.Soc.,**144,** L58,(1997).

19. D.H.Coleman, G.Zheng, B.N.Popov and R.E. White,J.Electrochem.Soc.,**143,** 1871(1995).
20. H.A. Durtee, D.M. See, B.N. Popov and R.E. White, J.Electrochem.Soc., **144**,2313 (1997).
21. R.N.Iyer, I. Takauchi, M.Zamanzadeh and H.W.Pickering, Corrosion, **46**,360(1990).
22. C.D. Kim and B.E. Wilde, J.Electrochem.Soc., **118**,202(1971).
23. J.O'.M. Bockris, J.L.Carbajal, B.R. Scharifker and K. Chandrasekaran, J. Electrochem. Soc., 1957, 134 (1987).

Table 1 Values of i_o, k_1, k_2 and k'' obtained on an iron membrane of thickness 0.25mm in 0.1N H_2SO_4 + 0.9N Na_2SO_4, at different iodide ion concentrations.

[I⁻], mM	i_o, A cm^{-2}	k_1, cm s^{-1}	k_2, mol cm^{-2} s^{-1}	k'', mol cm^{-2} s^{-1}
0	2.00×10^{-6}	1.25×10^{-6}	2.61×10^{-8}	5.21×10^{-11}
1	1.17×10^{-6}	7.31×10^{-7}	2.73×10^{-8}	9.28×10^{-11}
10	9.00×10^{-7}	5.62×10^{-7}	2.83×10^{-8}	1.11×10^{-10}
50	6.00×10^{-7}	3.75×10^{-7}	3.79×10^{-8}	1.96×10^{-10}

Figures Captions

Fig.1 The relation between the steady state hydrogen permeation current and the cathodic potential of the HER obtained on an iron membrane of thickness 0.25mm in 0.1N H_2SO_4 + 0.9N Na_2SO_4, at different iodide ion concentrations.

Fig.2 Tafel plots obtained on an iron membrane of thickness 0.25mm in 0.1N H_2SO_4 + 0.9N Na_2SO_4 at different iodide ion concentrations.

Fig 3 The relation between the steady state hydrogen permeation current, i_∞, and the square root of the recombination current, $\sqrt{i_r}$, obtained on an iron membrane in 0.1N H_2SO_4 + 0.9N Na_2SO_4, at different iodide ion concentrations.

Fig.4 The relation between the charging function, $i_c \exp(a\alpha\eta)$, and the steady state hydrogen permeation current, i_∞, for an iron membrane of thickness 0.25mm in 0.1N H_2SO_4 +0.9N Na_2SO_4, at different iodide ion concentrations.

Fig.5 The variation of the hydrogen surface coverage, θ_H, with the cathodic potential obtained on an iron membrane of thickness 0.25mm, in 0.1N H_2SO_4 + 0.9N Na_2SO_4, at different iodide ion concentrations

Fig.6 Hydrogen permeation transients obtained on an iron membrane of thickness 0.25mm in 0.5M Na_2SO_4 at a charging current density of 1.25mA cm^{-2} and different thiosulfate ion concentrations.

Fig.7 Tafel plots obtained on an iron membrane of thickness 0.25mm in 0.5 M Na_2SO_4 at different thiosulfate ion concentrations.

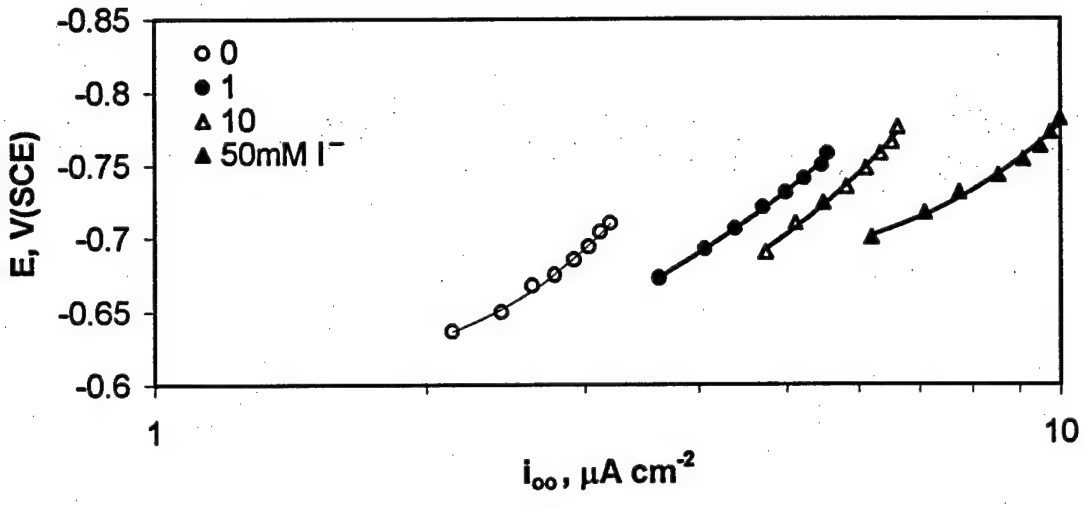

Fig.1 The relation between the steady state hydrogen permeation current and the cathodic potential of the HER obtained on an iron membrane of thickness 0.25mm in 0.1N H_2SO_4 + 0.9N Na_2SO_4, at different iodide ion concentrations.

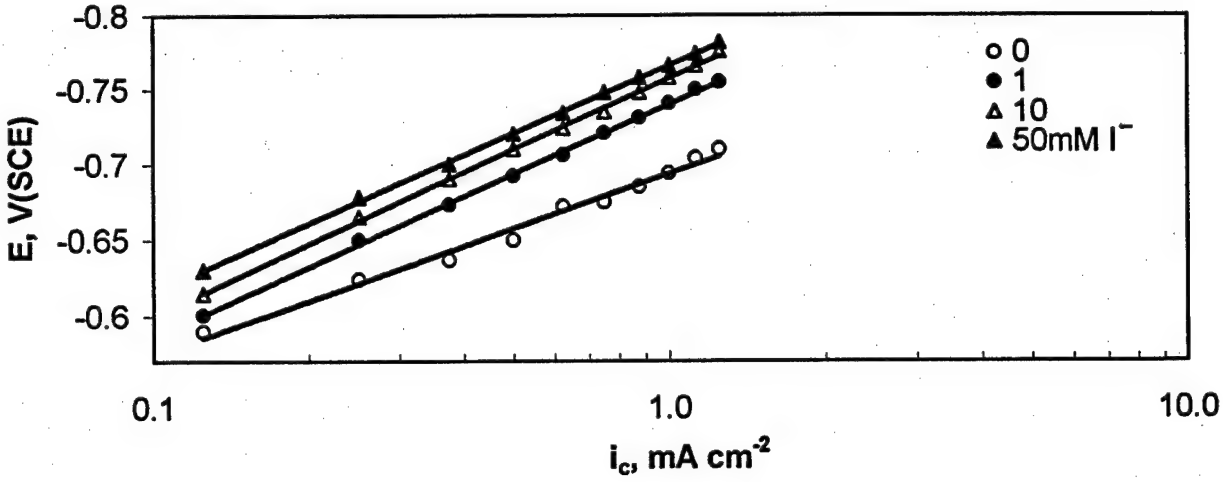

Fig.2 Tafel plots obtained on an iron membrane of thickness 0.25mm in 0.1N H_2SO_4 + 0.9N Na_2SO_4 at different iodide ion concentrations.

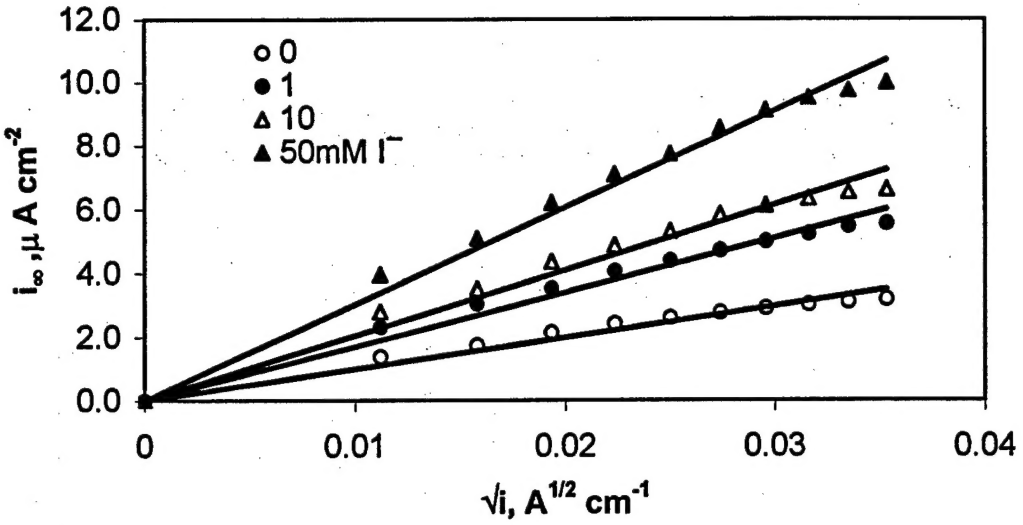

Fig 3 The relation between the steady state hydrogen permeation current, i_∞, and the square root of the recombination current, $\sqrt{i_r}$, obtained on an iron membrane in 0.1N H_2SO_4 + 0.9N Na_2SO_4, at different iodide ion concentrations.

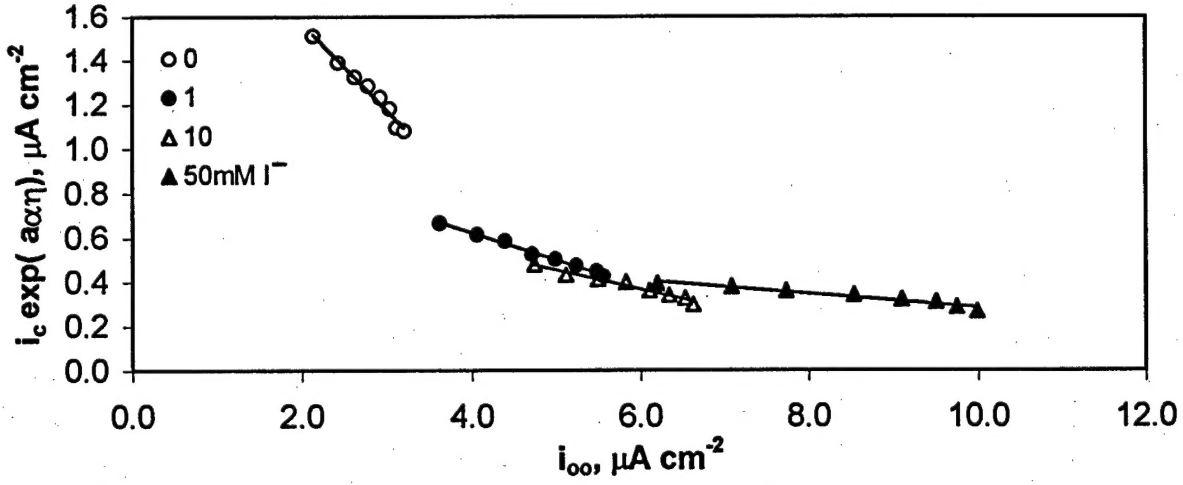

Fig.4 The relation between the charging function, $i_c \exp(a\alpha\eta)$, and the steady state hydrogen permeation current, i_∞, for an iron membrane of thickness 0.25mm in 0.1N H_2SO_4 +0.9N Na_2SO_4, at different iodide ion concentrations.

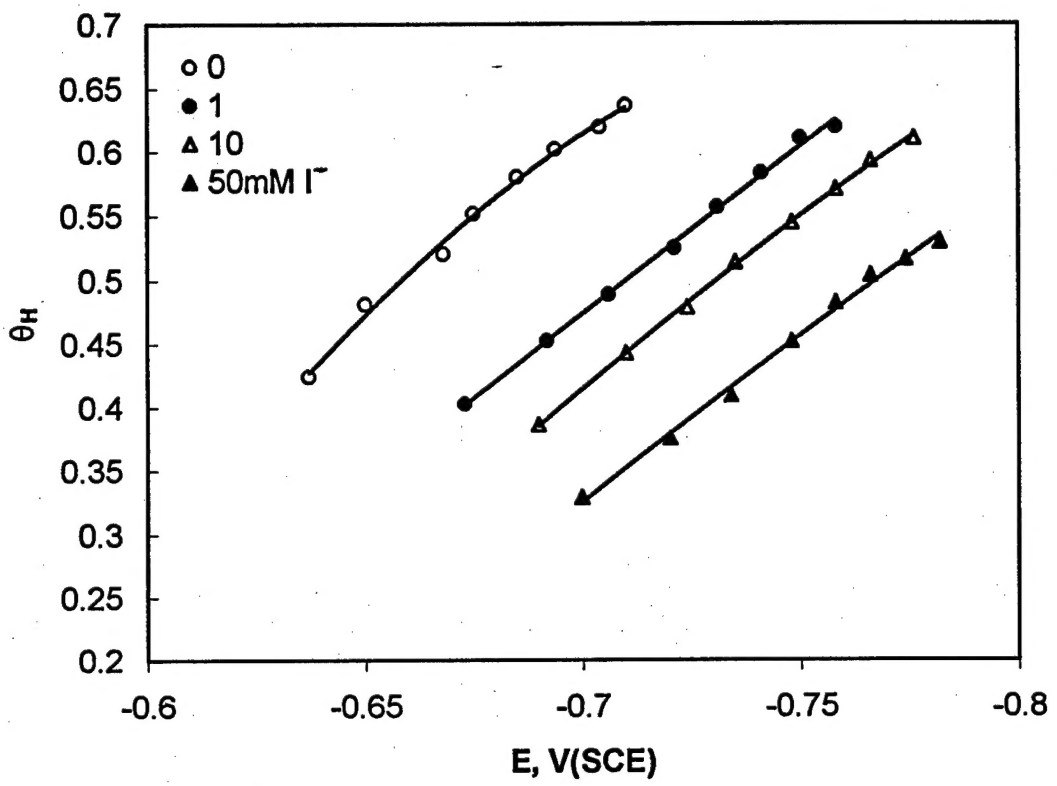

Fig.5 The variation of the hydrogen surface coverage, θ_H, with the cathodic potential obtained on an iron membrane of thickness 0.25mm, in 0.1N H_2SO_4 + 0.9N Na_2SO_4, at different iodide ion concentrations

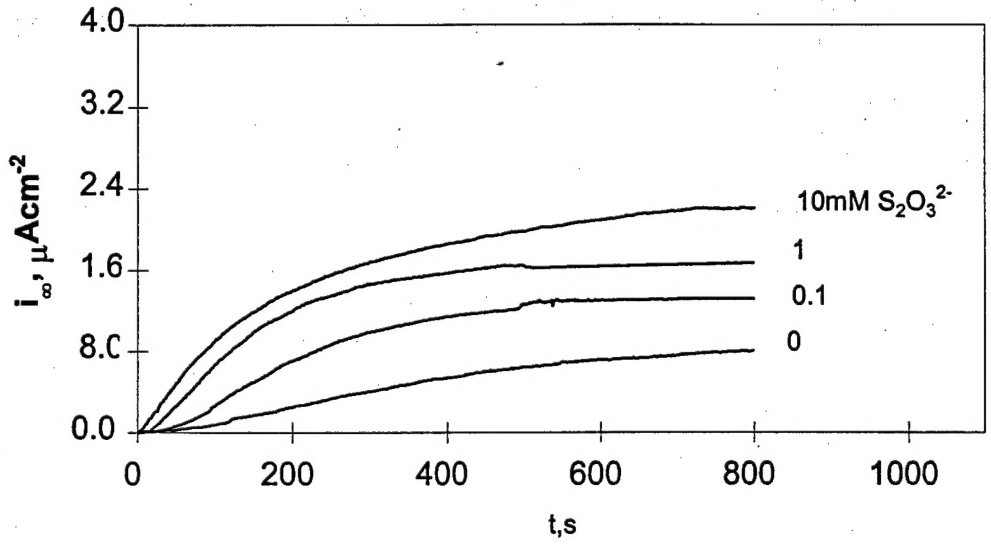

Fig.6 Hydrogen permeation transients obtained on an iron membrane of thickness 0.25mm in 0.5M Na_2SO_4 at a charging current density of 1.25mA cm^{-2} and different thiosulfate ion concentrations.

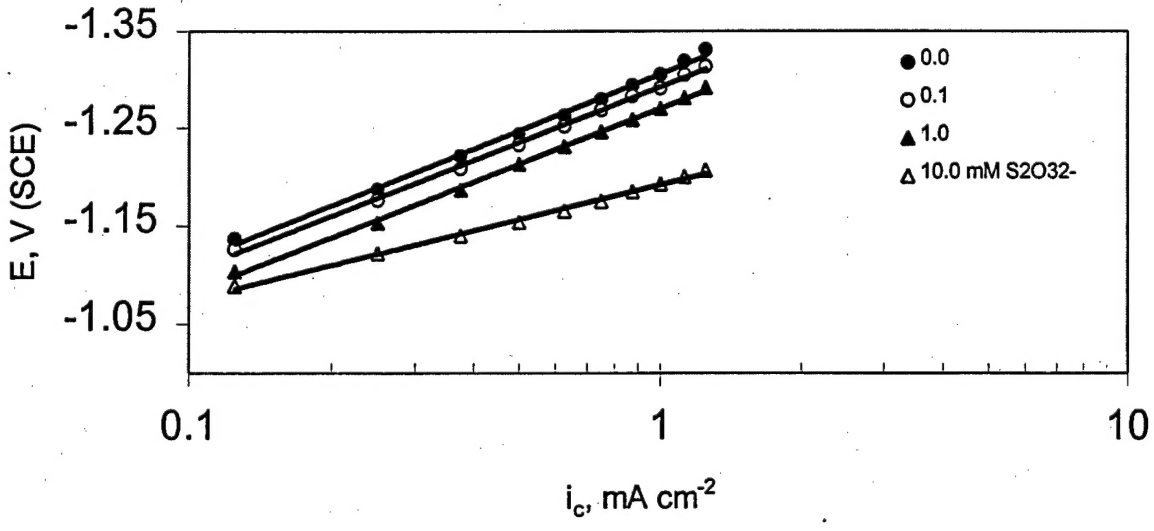

Fig.7 Tafel plots obtained on an iron membrane of thickness 0.25mm in 0.5 M Na_2SO_4 at different thiosulfate ion concentrations.

Reports Distribution

Addresses	Number of Copies
Office of Naval Research Program Officer John A. Sedriks ONR 332 Ballston Centre Tower One 800 North Quincy Street Arlington, VA 22217-5660	3
Administrative Grants Officer OFFICE OF NAVAL RESEARCH REGIONAL OFFICE CHICAGO 536 S. Clark Street Room 208 Chicago, IL 60605-1588	1
Director, Naval Research Laboratory Attn: Code 2627 4555 Overlook Drive Washington, DC 20375-5326	1
Defense Technical Information Center 8725 John J. Kingman Road STE 0944 Ft. Belvoir, VA 22060-6218	2